

Monolayer hydrodynamics:

Coupling between bulk flow and insoluble monolayers at a gas/liquid interface

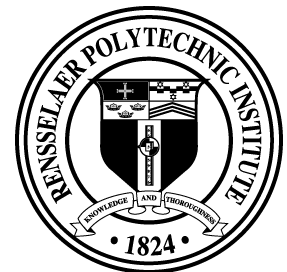
Amir H. Hirsaa

Mechanical & Aerospace Engineering

Also Chemical & Biological Engineering
(joint appointment)

Rensselaer Polytechnic Institute

•On sabbatic at UCSB (office: Engineering-II, Room 3337, tel. x7346)
hirsaa@rpi.edu



Outline of Lectures

- ✓ 1) Macroscopic description of monolayers
 - A) Introduction to surfactant monolayers, including applications
 - B) Constitutive relation for Newtonian interface: Boussinesq-Scriven surface model and coupling to Navier-Stokes equations
 - C) Elastic and viscous response of monolayers: Why surfactant monolayers are elastic
 - D) Consequences of surface elasticity, including examples
- 2) Intrinsic interfacial viscosities: Not a figment of chemists' imagination
 - A) Surface shear viscosity
 - B) Surface dilatational viscosity

the (bulk) stress tensor is:

$$\boldsymbol{\tau} = \left(-p + \overbrace{\left(\mu' - \frac{2}{3}\mu \right)}^{\lambda \text{ (second coefficient of viscosity)}} \right) \text{div } \mathbf{u} + 2\mu \mathbf{D}$$

Note that the bulk viscosity, given by $\mu' = \lambda + \frac{2}{3}\mu$

The surface stress tensor is analogous and is given by:

$$\mathbf{T}^s = (\sigma + (\kappa^s - \mu^s) \text{div}_s \mathbf{u}^s) \mathbf{I}^s + 2\mu^s \mathbf{D}^s$$

Comparison between the variables and properties of bulk flow and surface flow

Flow Properties/Variables	Bulk	Surface
x -velocity	u	u^s
y -velocity	v	v^s
rate of deformation tensor	\mathbf{D}	\mathbf{D}^s
pressure	p	$-\sigma$
coefficient of shear viscosity	μ	μ^s
coefficient of dilatational viscosity	μ'	κ^s

Boundary conditions for equations of motion

In the presence of surfactant monolayers, boundary conditions for Navier-Stokes equations are functions of intrinsic interfacial properties

For a Newtonian gas/liquid interface, the surface stress tensor is

$$\mathbf{T}^s = \sigma \mathbf{I}_s + \mathbf{S}^s = (\sigma + (\kappa^s - \mu^s) \operatorname{div}_s \mathbf{u}^s) \mathbf{I}_s + 2 \mu^s \mathbf{D}^s,$$

where the viscous part of the surface stress tensor, \mathbf{S}^s , is a linear function of the surface rate of deformation tensor, \mathbf{D}^s

“**Boussinesq-Scriven surface model**”

Intrinsic interfacial properties:

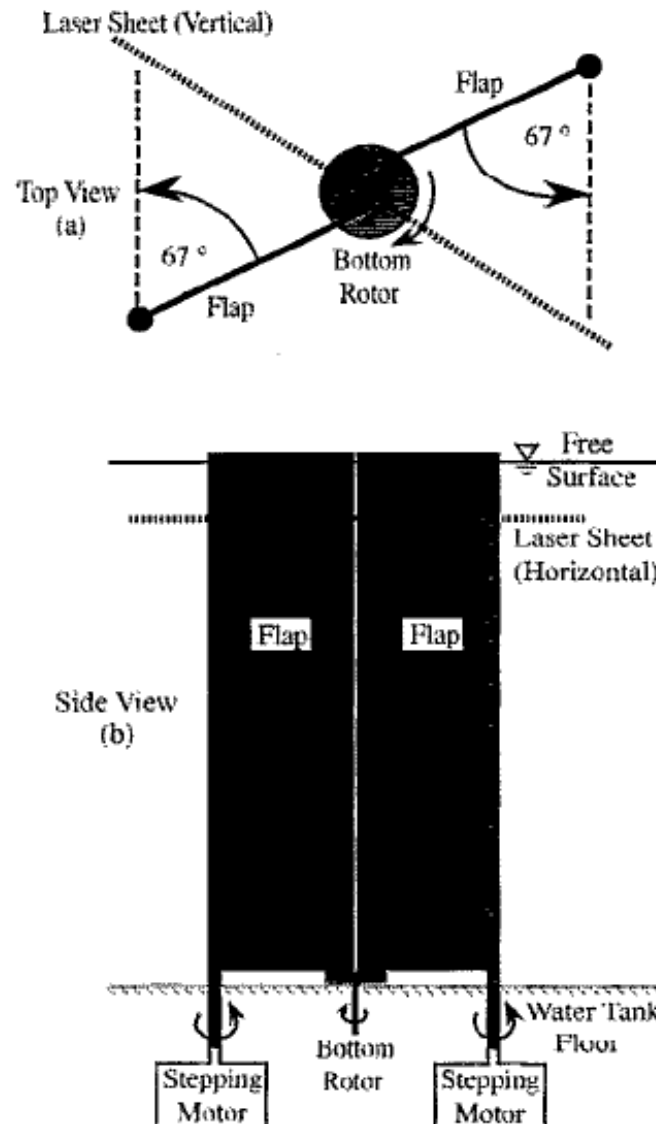
1. σ thermodynamic (equilibrium surface tension)
2. μ^s surface shear viscosity
3. κ^s surface dilatational viscosity

e.g., for planar flow at flat interface, the x-component yields:

$$\mu \frac{\partial u}{\partial y} \Big|_{y=0} = \frac{\partial \sigma}{\partial x} + \frac{\partial}{\partial x} \left[(\kappa^s - \mu^s) \frac{\partial u^s}{\partial x} \right]$$

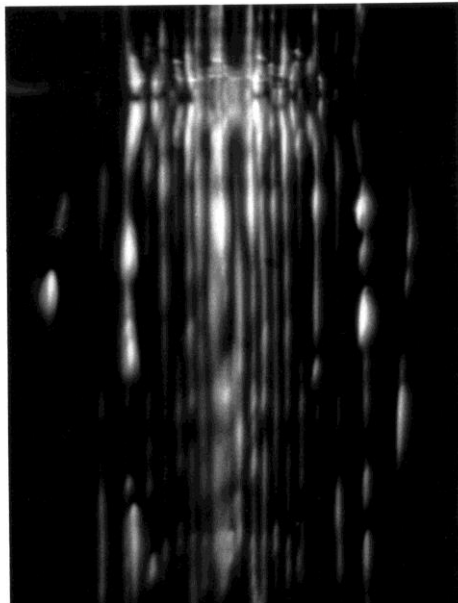
first seminar

Experimental set-up to demonstrate μ^s



Boussinesq-Scriven surface model: μ^s

Clean interface
or
monolayer with small μ^s



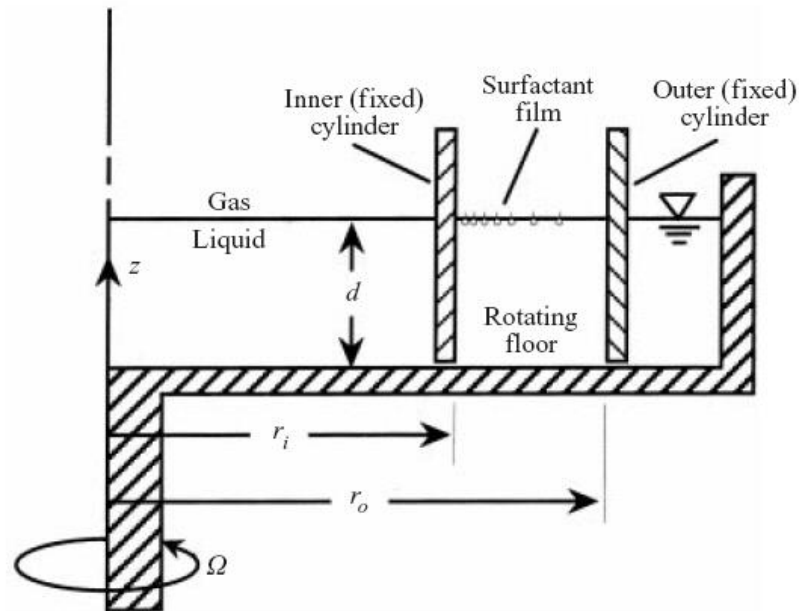
$\text{Re}_\Gamma \approx 10^3$
($L \approx 0.1$ m)

monolayer with large μ^s



The significance is the scale at which these effects are documented

Direct determination of $\mu^s(c)$



Note, this is an extension of a technique introduced by Mannheimer & Schechter (1970)

Numerical simulation of Navier-Stokes with Boussinesq-Scriven surface model

non-dimensional velocity vector is

$$\mathbf{U} = (u, v, w) = \left(-\frac{1}{r} \frac{\partial \psi}{\partial z}, \frac{\alpha}{r}, \frac{1}{r} \frac{\partial \psi}{\partial r} \right), \quad \begin{array}{l} \text{Stokes streamfunction, } \psi \\ \text{axial angular momentum, } \alpha = rv \end{array}$$

and the corresponding vorticity vector is

$$\nabla \times \mathbf{U} = \left(-\frac{1}{r} \frac{\partial \alpha}{\partial z}, \eta, \frac{1}{r} \frac{\partial \alpha}{\partial r} \right).$$

The use of ψ and α is convenient in axisymmetric swirling flows; contours of ψ in an (r, z) -plane depict the streamlines of the flow, and contours of α in that plane depict the vortex lines.

We use r_o as the length scale and $1/\Omega$ as the time scale, and define a Reynolds number $Re(= \Omega r_o^2/\nu)$ to non-dimensionalize the axisymmetric Navier–Stokes equations:

$$\frac{D\alpha}{Dt} = \frac{1}{Re} \nabla_*^2 \alpha, \quad (2.1)$$

$$\frac{D\eta}{Dt} + \frac{\eta}{r^2} \frac{\partial \psi}{\partial z} - \frac{1}{r^3} \frac{\partial \alpha^2}{\partial z} = \frac{1}{Re} \left(\nabla^2 \eta - \frac{\eta}{r^2} \right), \quad (2.2)$$

where

$$\nabla_*^2 \psi = -r\eta, \quad (2.3)$$

$$\frac{D}{Dt} = \frac{\partial}{\partial t} - \frac{1}{r} \frac{\partial \psi}{\partial z} \frac{\partial}{\partial r} + \frac{1}{r} \frac{\partial \psi}{\partial r} \frac{\partial}{\partial z},$$

$$\nabla^2 = \frac{\partial^2}{\partial z^2} + \frac{\partial^2}{\partial r^2} + \frac{1}{r} \frac{\partial}{\partial r},$$

and

$$\nabla_*^2 = \frac{\partial^2}{\partial z^2} + \frac{\partial^2}{\partial r^2} - \frac{1}{r} \frac{\partial}{\partial r}.$$

In our previous studies of this system (Lopez & Hirs 2000; Hirs *et al.* 2001) we treated the interface following Scriven (1960), except that we allowed the surface viscosities to vary with the surfactant concentration. For a flat interface, only the tangential stress balance plays a dynamic role. The tangential stress balance in the azimuthal direction is

$$\frac{\partial v}{\partial z} = \hat{\mu}^s \left(\frac{\partial^2 v}{\partial r^2} + \frac{1}{r} \frac{\partial v}{\partial r} - \frac{v}{r^2} \right) + \frac{\partial \hat{\mu}^s}{\partial r} \left(\frac{\partial v}{\partial r} - \frac{v}{r} \right), \quad (2.4) \quad 9$$

and in the radial direction

$$\eta = \frac{1}{Ca} \frac{\partial \sigma}{\partial r} + (\hat{\mu}^s + \hat{\kappa}^s) \left(\frac{1}{r^2} \frac{\partial^2 \psi}{\partial r \partial z} - \frac{1}{r} \frac{\partial^3 \psi}{\partial r^2 \partial z} \right) - \frac{1}{r} \frac{\partial^2 \psi}{\partial r \partial z} \frac{\partial(\hat{\mu}^s + \hat{\kappa}^s)}{\partial r} + \frac{2}{r^2} \frac{\partial \psi}{\partial z} \frac{\partial \hat{\mu}^s}{\partial r}, \quad (2.5)$$

where $Ca (= \mu \Omega r_o / \sigma_0)$ is the capillary number, $\hat{\mu}^s = \mu^s / \mu r_o$ and $\hat{\kappa}^s = \kappa^s / \mu r_o$.

We have found that when the surface has an adequate amount of surfactant, the radial component of velocity on the interface is zero, and the interfacial condition in the radial direction reduces to no-slip, regardless of the physicochemical details of the system (Lopez & Hirs 2000; Hirs *et al.* 2001). Thus, instead of (2.5), we have

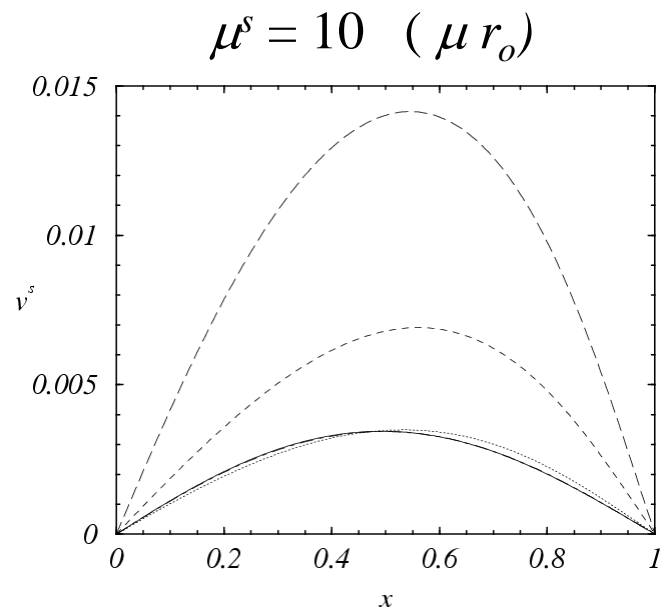
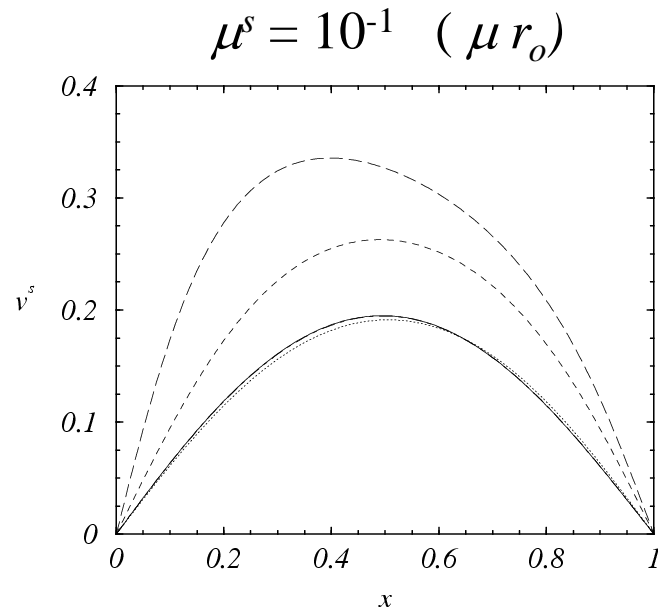
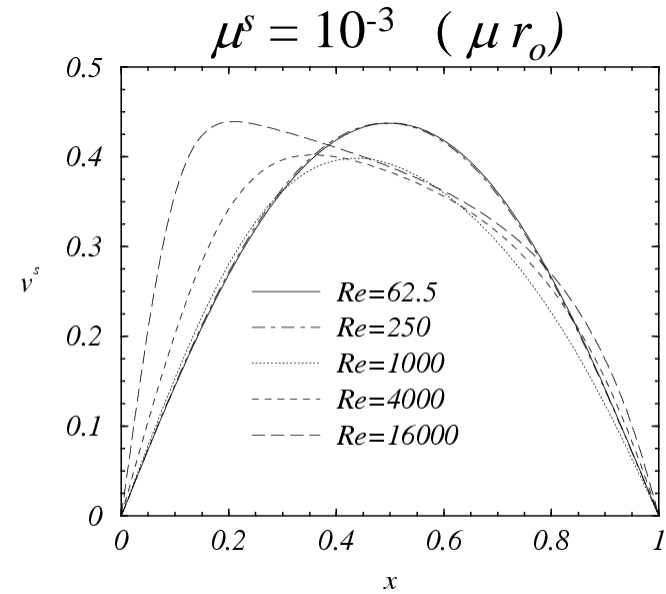
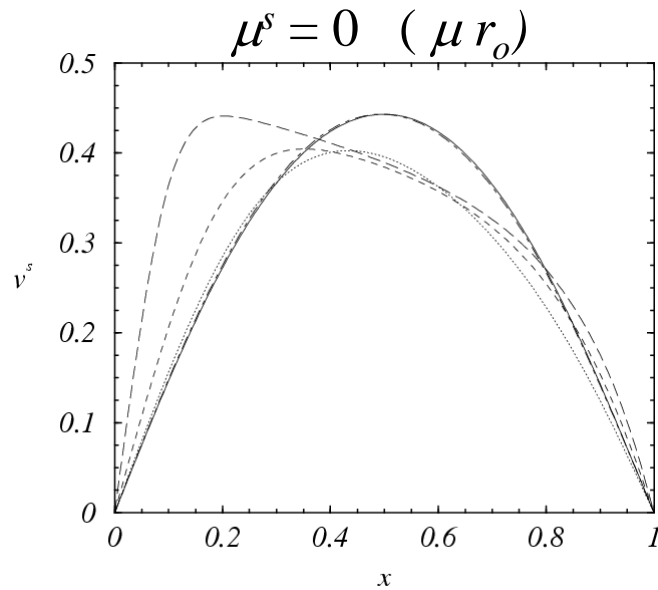
$$\eta = -\frac{1}{r} \frac{\partial^2 \psi}{\partial z^2} = \frac{\partial w}{\partial z}. \quad (2.6)$$

With the interface suitably covered by the monolayer and the radial surface velocity zero, we neglect any surface concentration gradients. This means that there is no need to solve an advection–diffusion equation for monolayer concentration, and the surface shear viscosity at such an interface is also constant since the concentration is uniform. This allows us to reduce (2.4) to

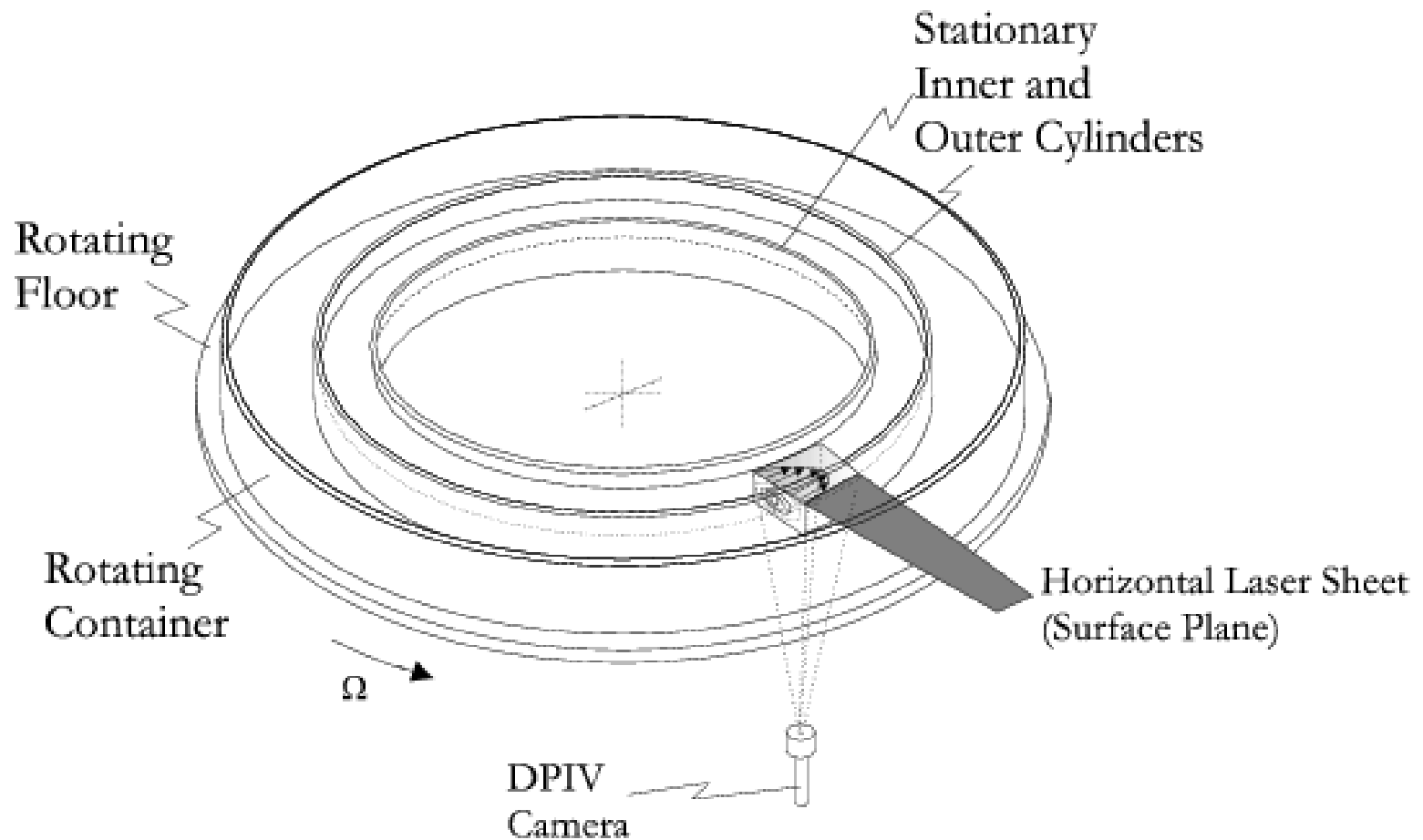
$$\frac{\partial v}{\partial z} = \hat{\mu}^s \left(\frac{\partial^2 v}{\partial r^2} + \frac{1}{r} \frac{\partial v}{\partial r} - \frac{v}{r^2} \right). \quad (2.7)$$

Now the only interfacial parameter in the system is the surface shear viscosity. In the Mannheimer & Schechter (1970) inertialess theory, this is also true, but here the essential difference is that the inertia of the system redistributes the vortex lines and so the v -profile at the interface requires the solution of the Navier–Stokes equations. However, as in the Stokes limit, we need only measure the azimuthal velocity at the interface to determine μ^s .

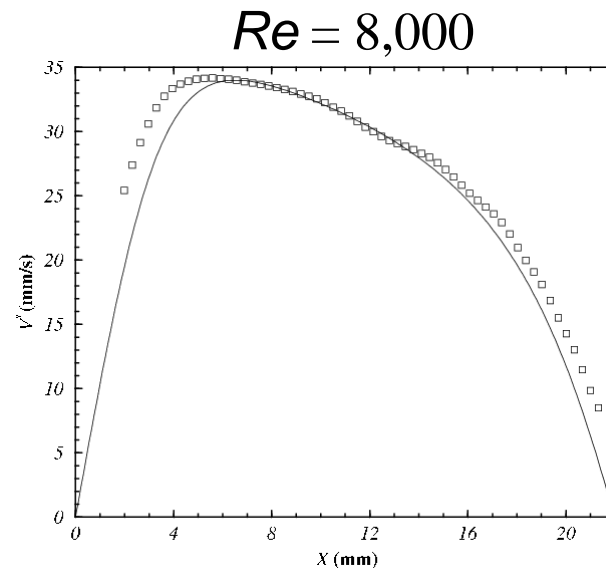
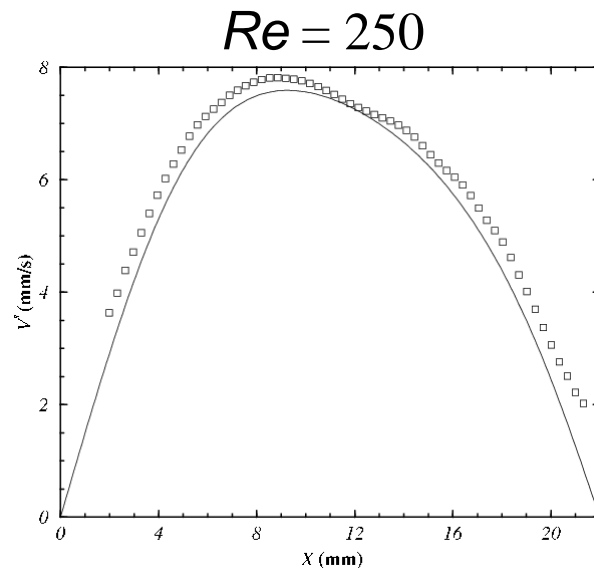
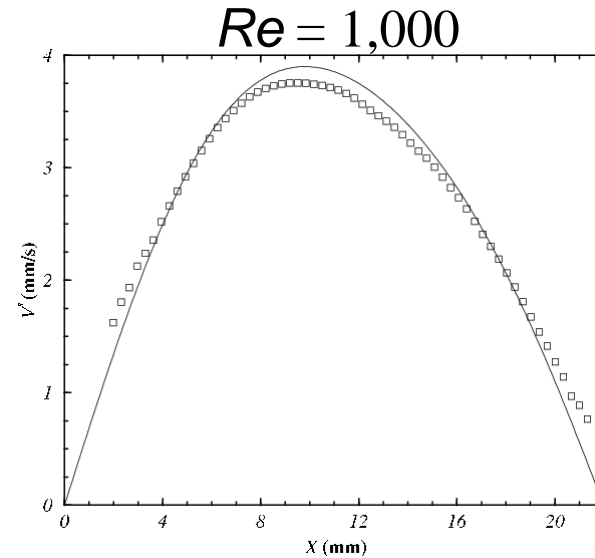
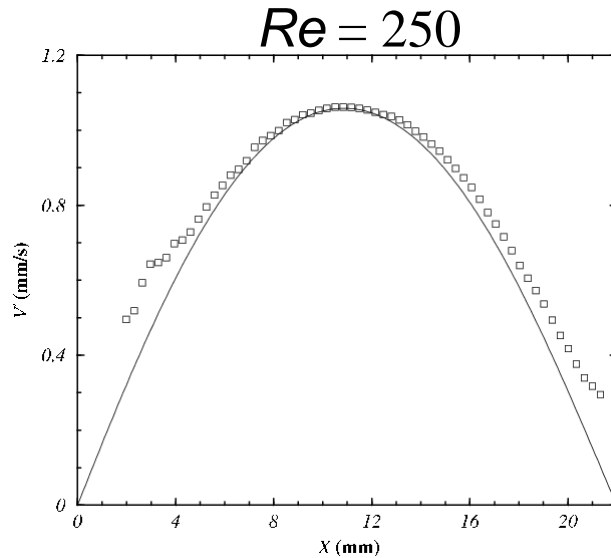
Computed tangential velocity profiles for various Re and μ^s



Experimental apparatus



Measured velocity for a stearic acid monolayer ($c = 0.8 \text{ mg/m}^2$)
compared to prediction for a fixed $\mu^s (=0.006 \mu r_o)$



Note a single value of μ^s fits measurements over many decades of shear rate

Non-Newtonian behavior observed with hemicyanine monolayer

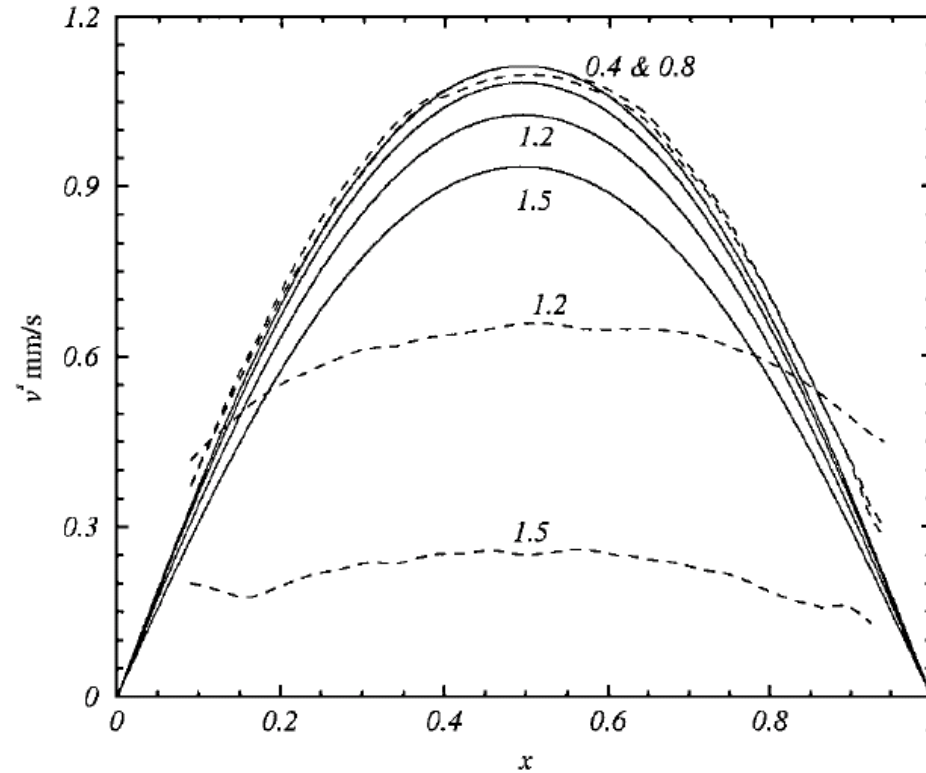


FIG. 5. Azimuthal velocity profiles at the interface driven with $Re = 250$ for C_0 mg/m² as indicated; broken lines are measurements using DPIV and the solid lines are computed.

“Thixotropic” behavior (due to homogenization at meso-scale?)

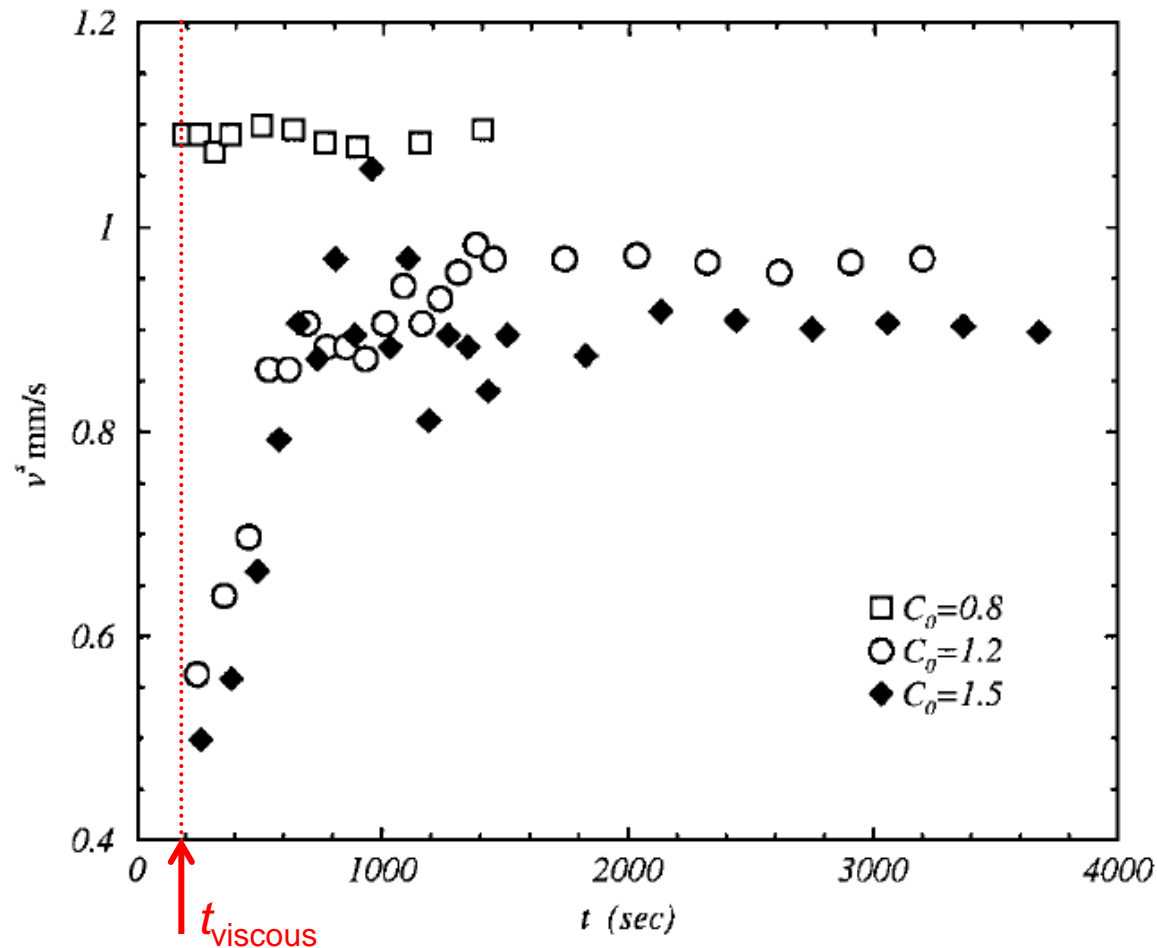


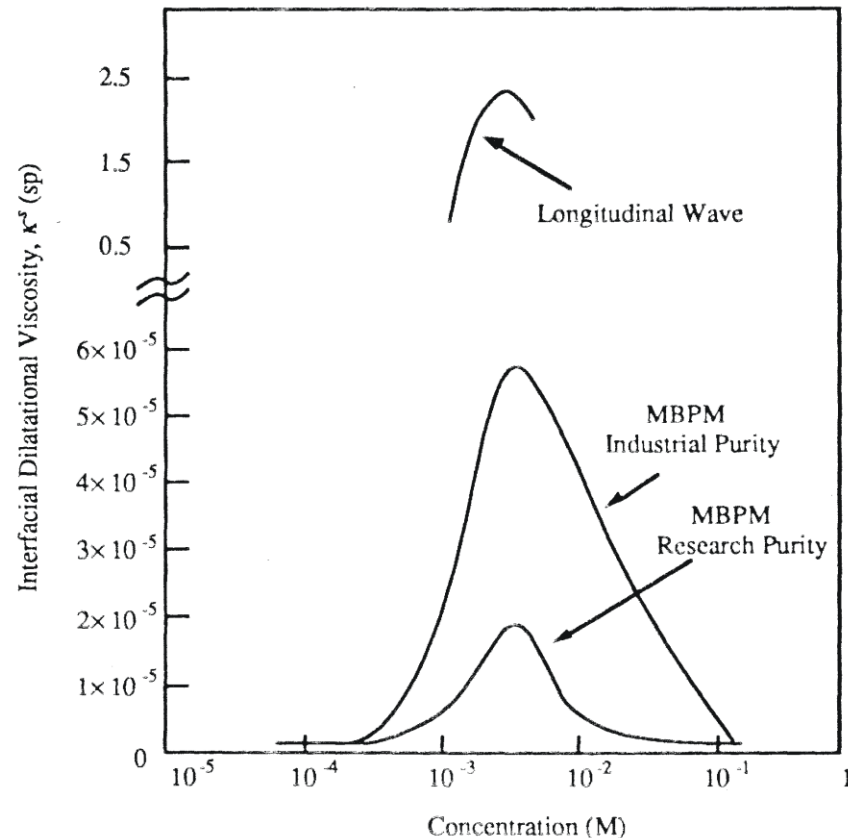
FIG. 9. Centerline azimuthal velocity measured in a conventional deep-channel viscometer vs time (in seconds) following the startup of the floor rotation, for an air/water interface with a hemicyanine monolayer of surface concentration as indicated (in mg/m^2).

Boussinesq-Scriven surface model: $\kappa^s(c)$

σ is straightforward to measure & its effect (Marangoni) understood at SS
 μ^s consistent measurements of μ^s reported (at least at scales ≥ 1 cm)
 κ^s is not well understood

Vastly different results reported for a given (soluble) surfactant

Negative values reported by several groups, for both soluble and insoluble monolayers



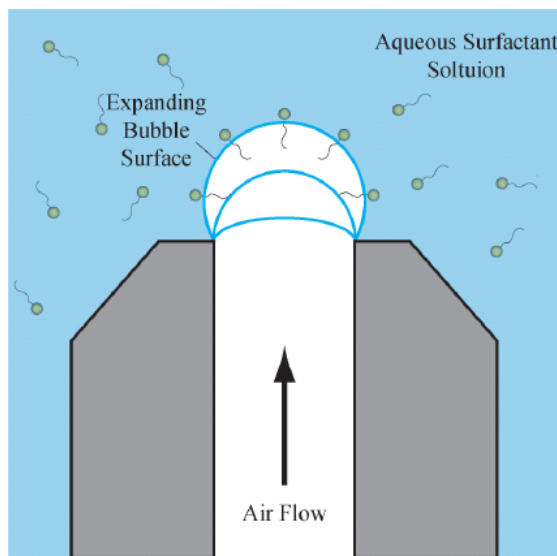
- Sharpe & Estoe
- Peace & Richards
- Sharp & Earnshaw
- Peace & Richards
- Monroy et al.
- Langevin et al.
- He et al.
- Monroy et al.

Lopez et al.

- Langmuir* (1996)
- Polymer* (1996)
- J Chemical Phys* (1997)
- Langmuir* (1998)
- Coll. & Surf. A* (1998)
- PRE* (1998)
- Coll. & Surf. A* (2002)
- J Phys Chem B* (2002)
- PRE* (2004)

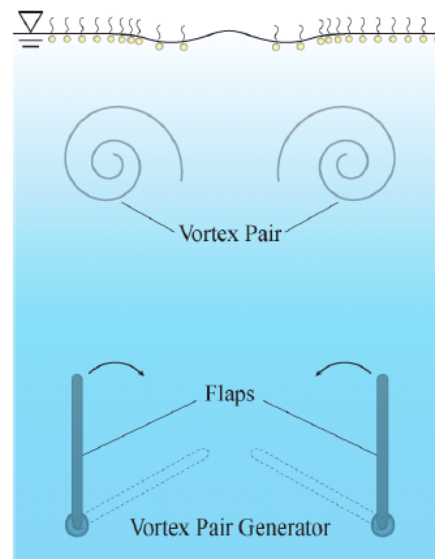
Some previous surface dilatational viscometers

Maximum Bubble
Pressure Method
(soluble systems only)



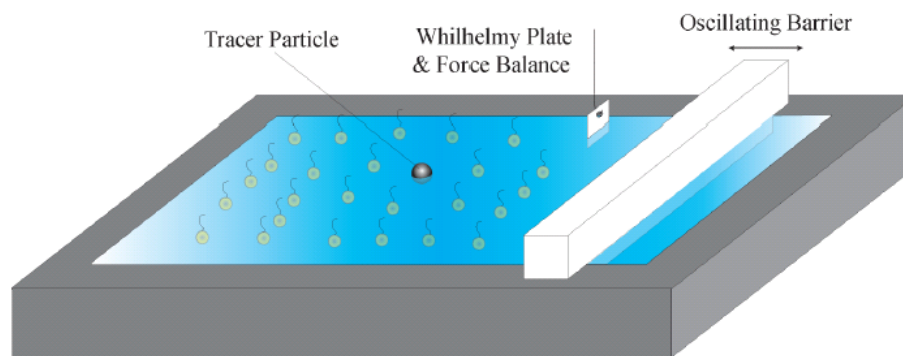
(a)

Vortex Pair Method
(requires measurement
of $c(t)$ – not easy – and
lacks periodicity)



(b)

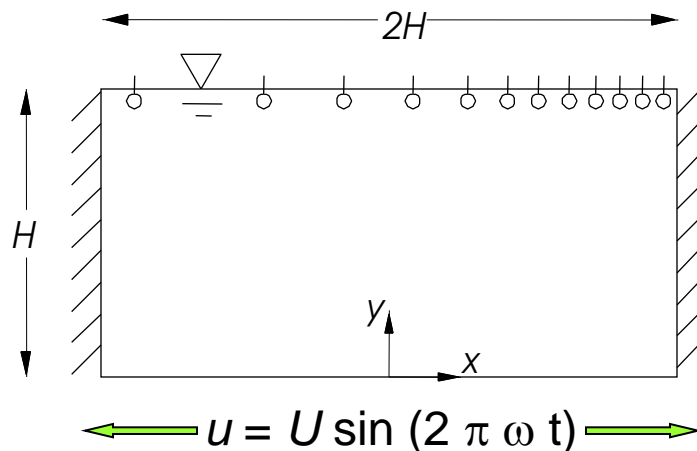
Longitudinal Wave
Method
(can be dominated
by Marangoni effect)



(c)

“New” surface (dilatational) viscometer

Open cavity with oscillating floor



$$Re = UH / \nu$$

$$St = \omega H^2 / \nu$$

where U is the maximum velocity of the floor

ω oscillation frequency (rad/s)

ν kinematic viscosity

Advantage: compressing/dilating monolayer with flow (vs. barrier, as in the “Longitudinal Wave Method”) allows the system to be driven fast without introducing transverse waves, preventing surface viscosity effect from being masked by surface elasticity

Also, H can be made “small” to accentuate effect of surface viscosity relative to surface elasticity (Marangoni effect)

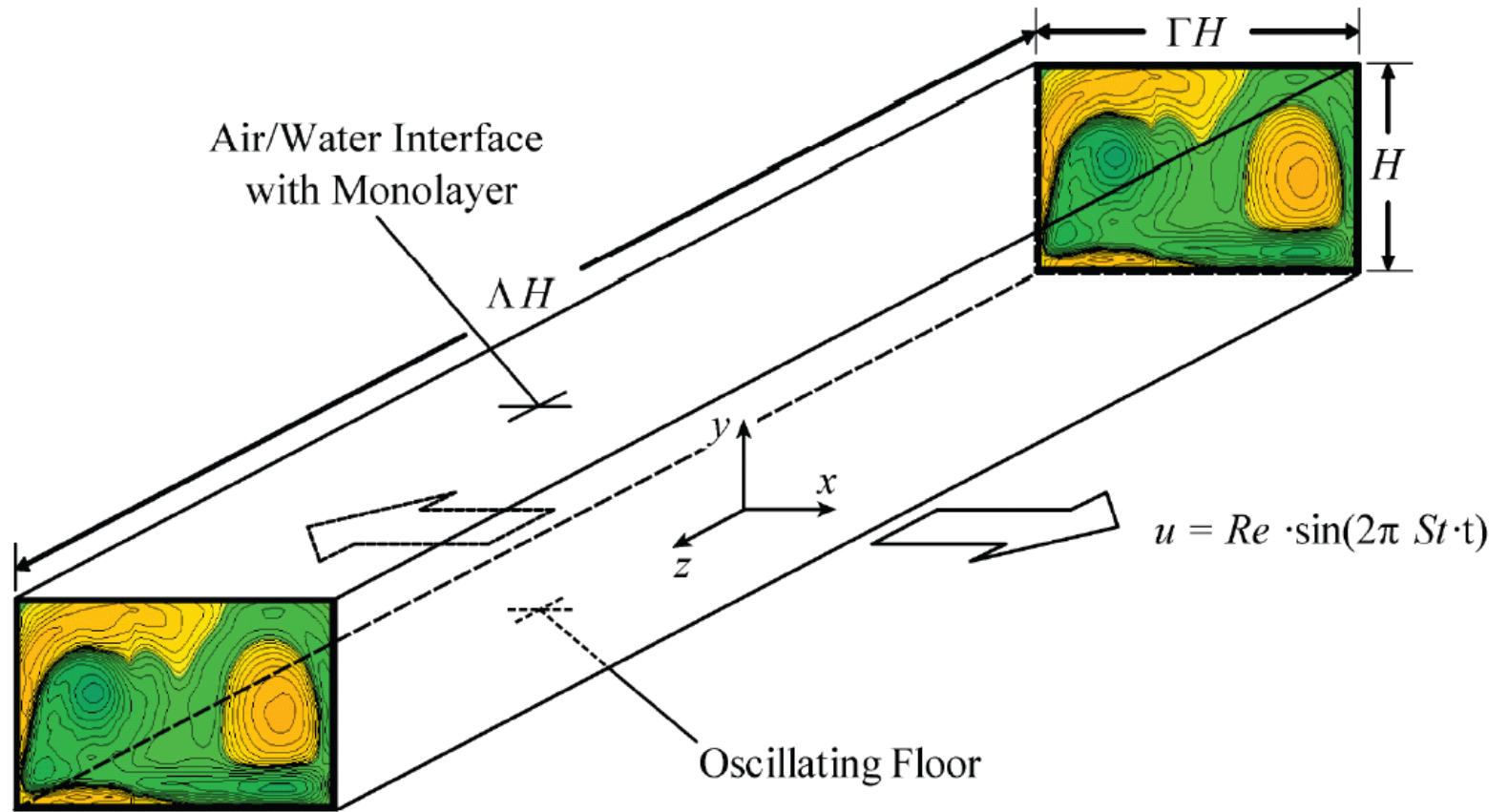
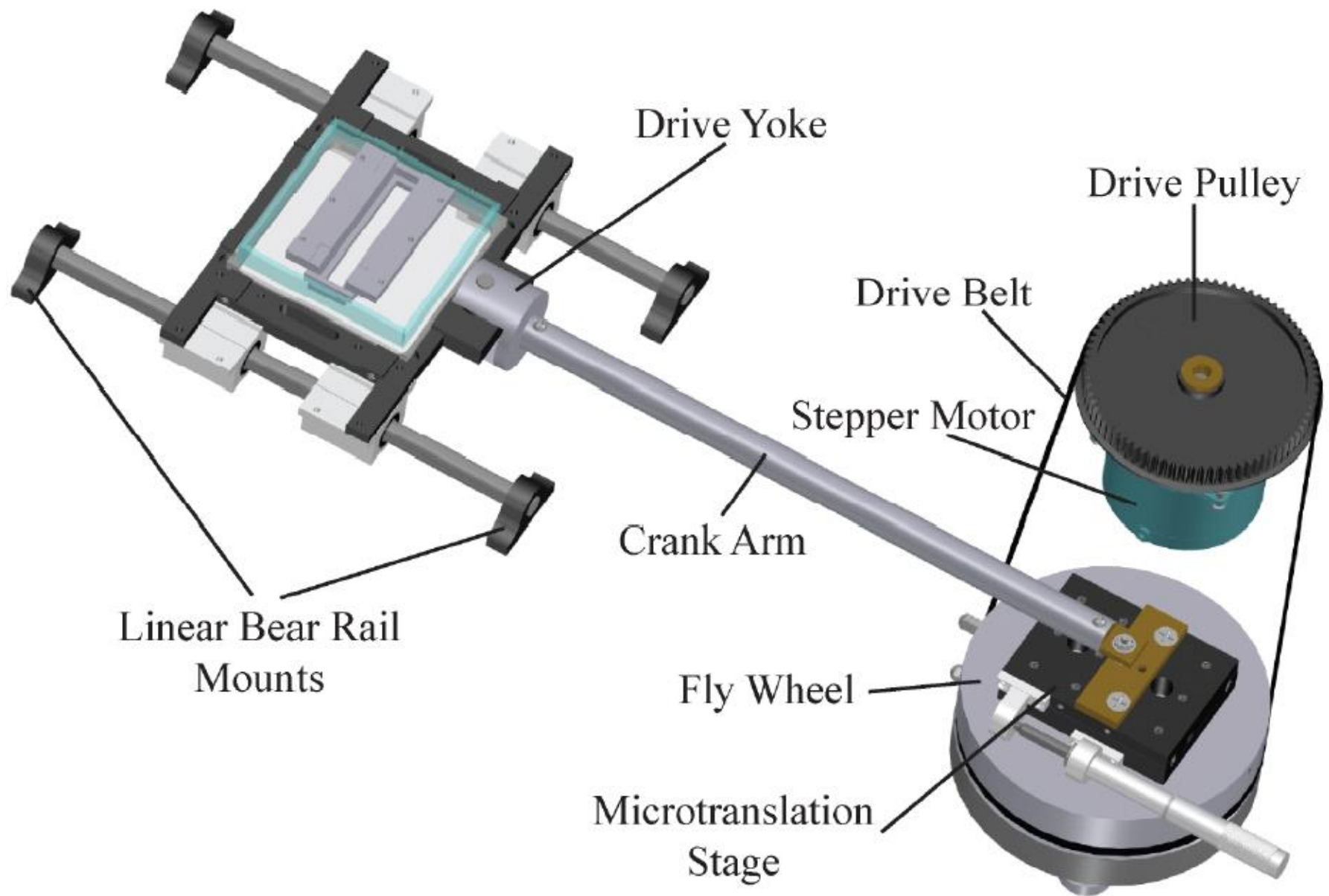


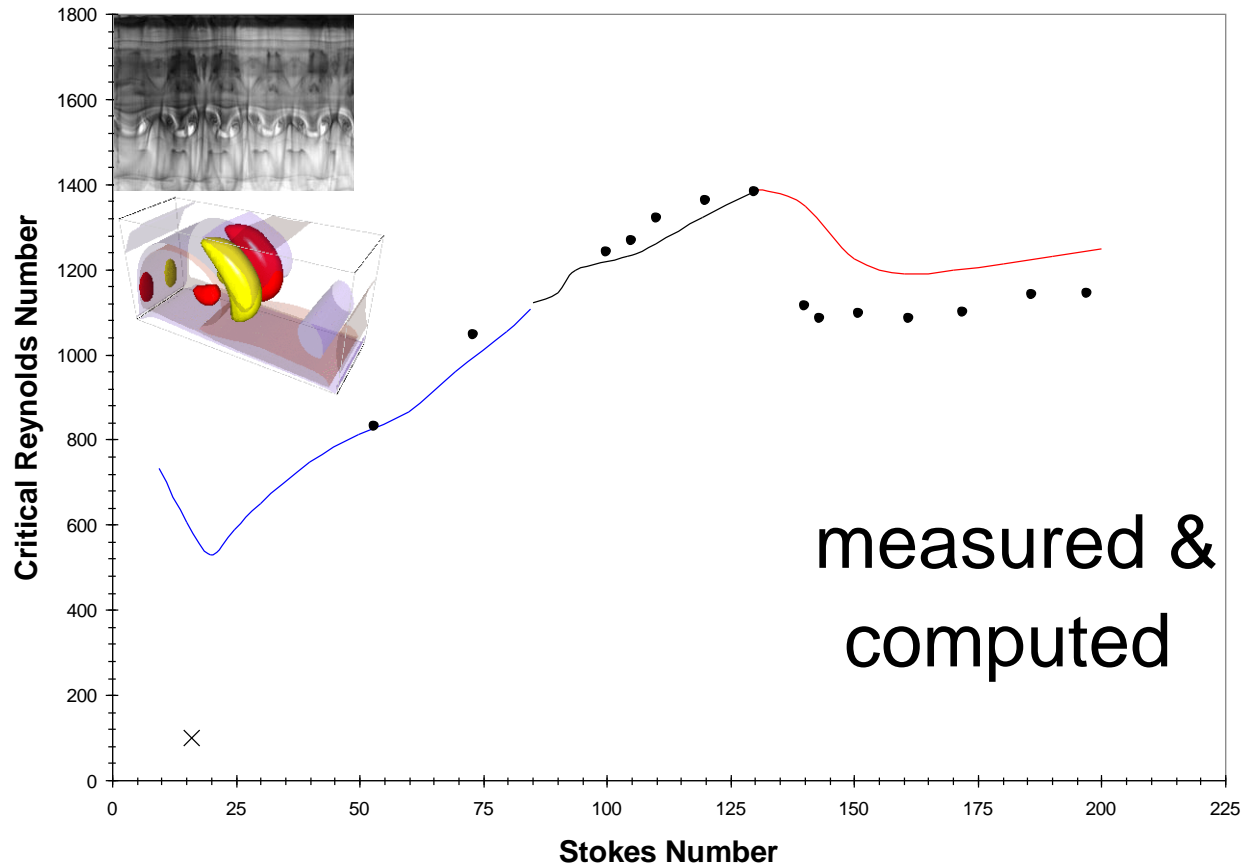
Figure 2.7: Diagram of the current experimental geometry consisting of a high aspect ratio (span to depth) open-top rectangular cavity in which the bulk flow is driven by the sinusoidal motion of the floor in its own plane. The superimposed color contour plots of the vorticity are taken from Vogel et al. [44].



Note: R_e can be controlled to better than 1 part in 1000

Stability limits of the driven cavity

onset of 3-dimensional disturbances



X original computations
of surface viscometer
(Lopez & Hirs 1999)

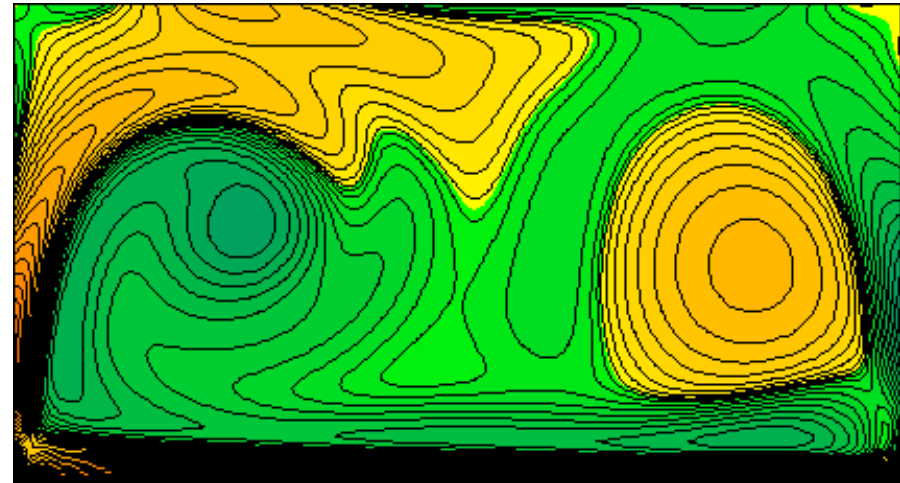
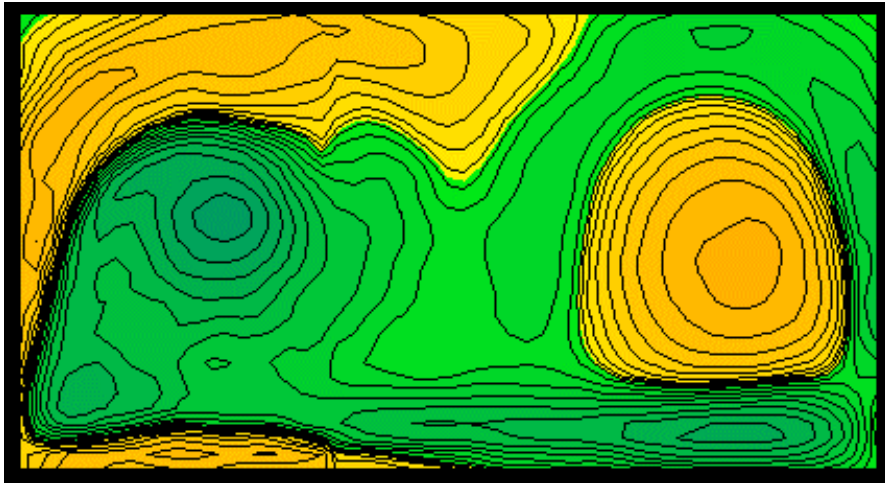
Refs.

Vogel, Hirs & Lopez *JFM* (2003)
Blackburn & Lopez *JFM* (2003)
Leung et al. *PRE* (2005)

2-D flow confirmation

Measurements
(DPIV)

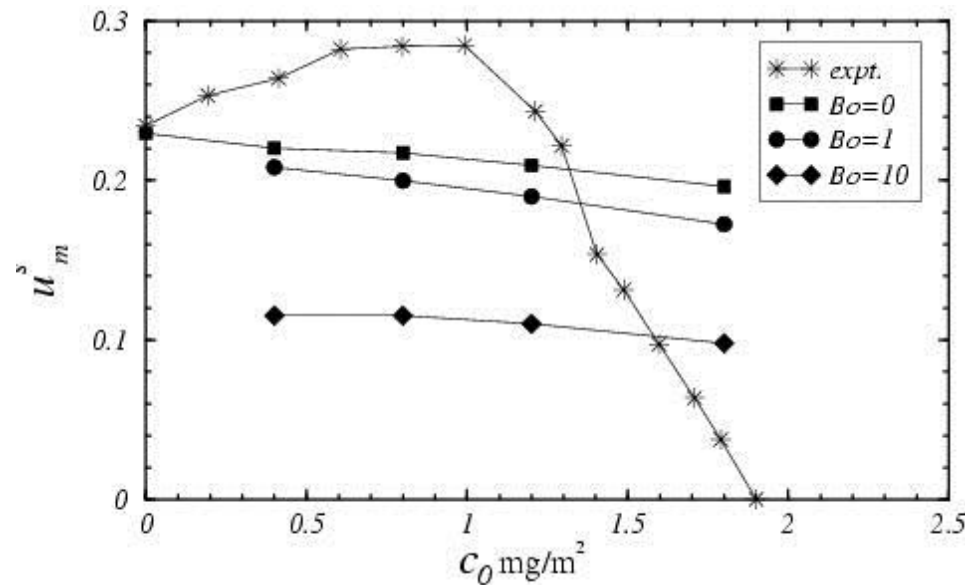
vs. Computations
(2-D Navier-Stokes)



Contours of z-vorticity, for the rigid top case
at phase $(t - NT) = 0$, for $Re = 747$, $St = 53$

Measured and computed x-velocity of the free surface with monolayer

(stearic acid at $Re = 498$ and $St = 53$)



Navier-Stokes were solved with Boussinesq-Scriven surface model, for various Boussinesq numbers:

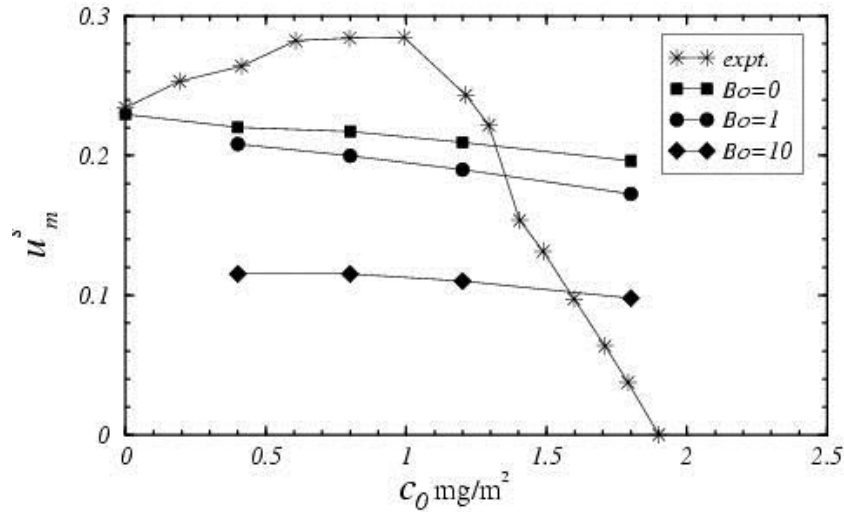
$$Bo = \frac{\kappa^s + \mu^s}{\mu H}$$

Measured (via boundary-fitted DPIV) and computed maximum x-velocity of the surface at the mid-point ($x = 0$, $y = H$) surface velocity.

Note the apparent negative value of Bo (and hence κ^s) over a wide range of concentrations

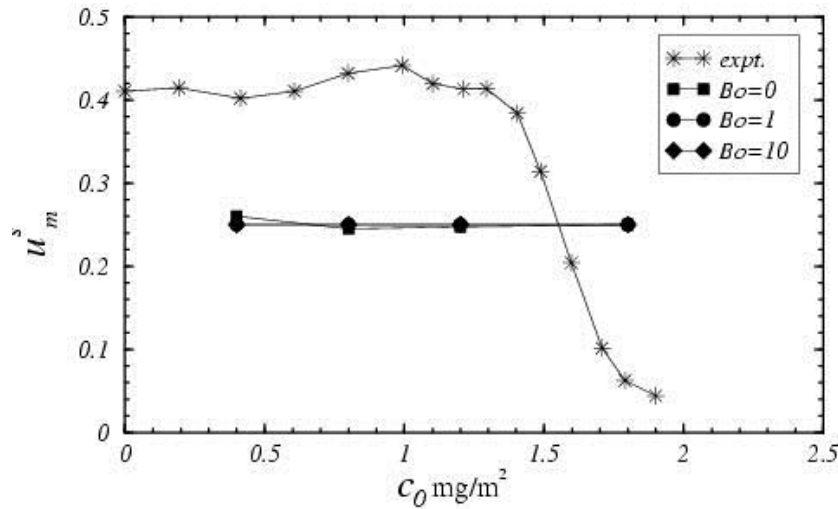
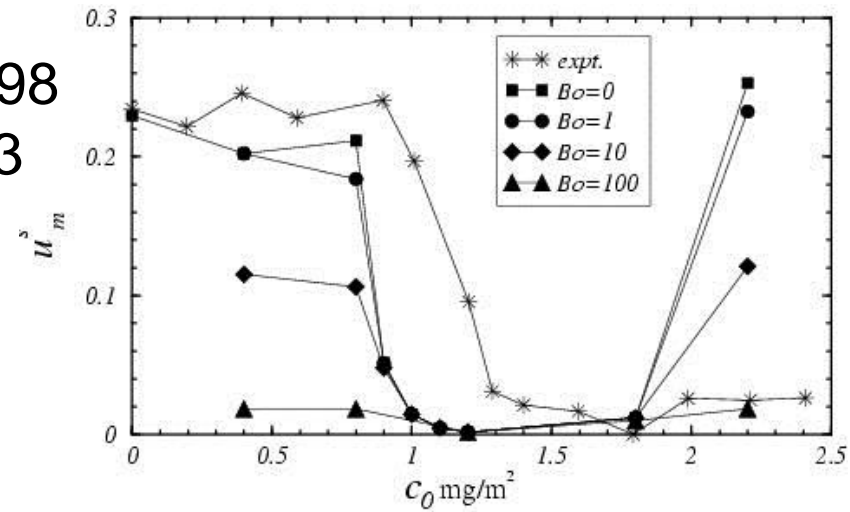
Also note the large value of κ^s at large concentrations

Stearic acid

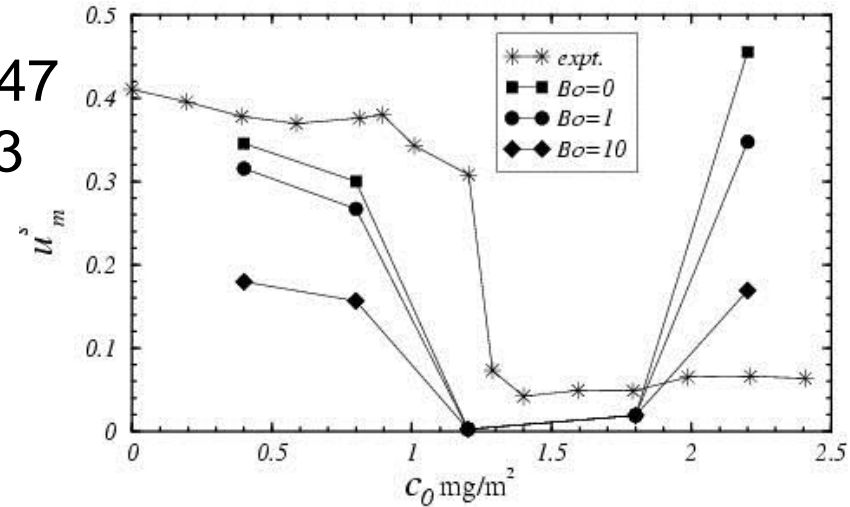


$Re = 498$
 $St = 53$

Vitamin K₁



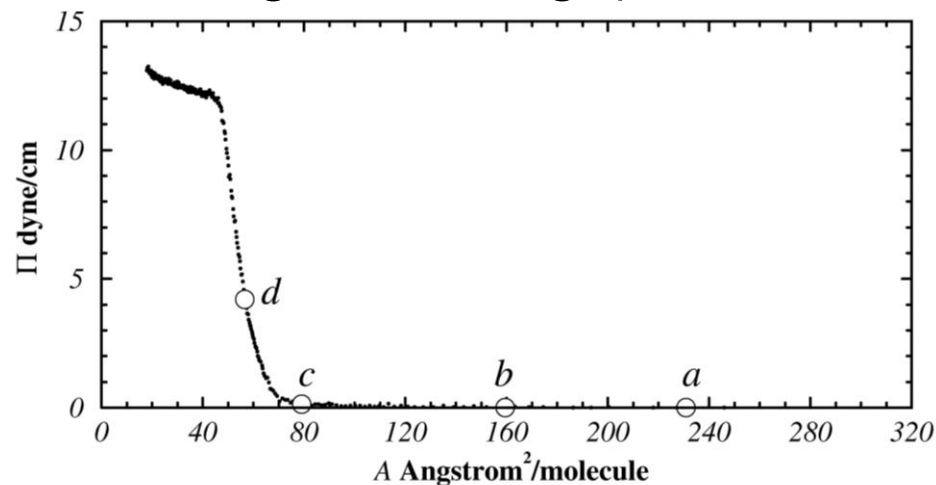
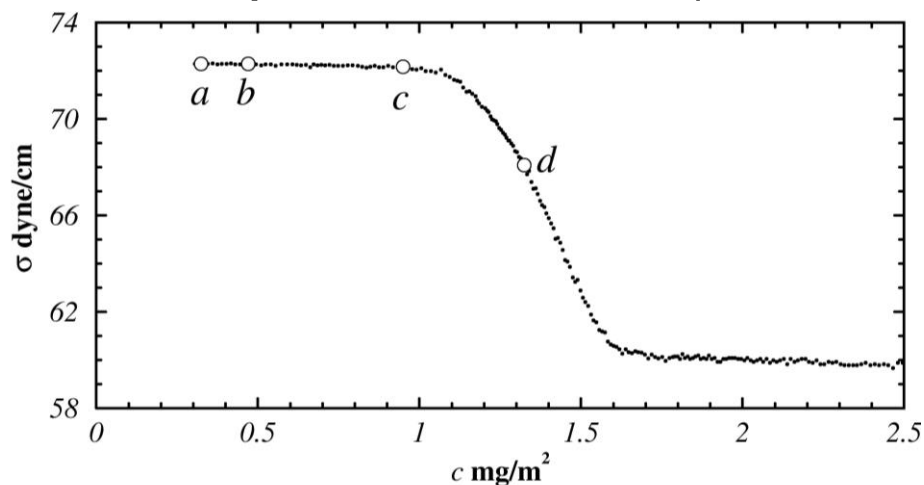
$Re = 747$
 $St = 53$



Note similar results for different monolayers, frequencies, and driving amplitudes

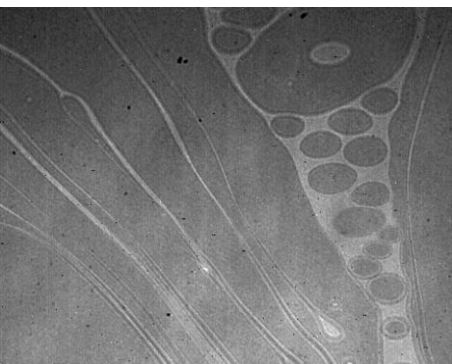
Relation between the anomaly and co-existing monolayer phases

Equation of state (measured in Langmuir trough)

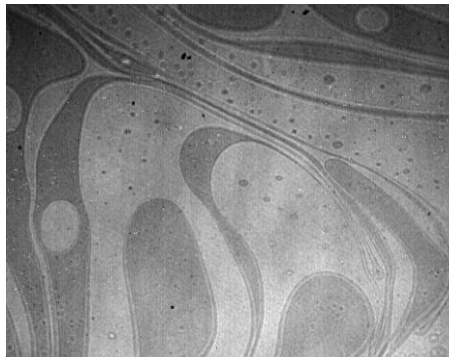


Brewster angle microscope (BAM) images

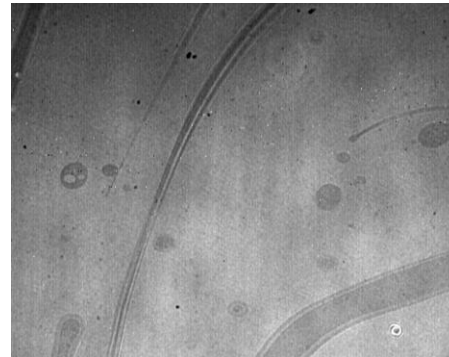
(a) $c = 0.32$ mg/m²



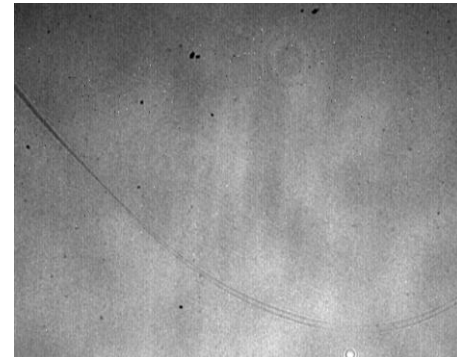
(b) $c = 0.47$ mg/m²



(c) $c = 0.95$ mg/m²



(d) $c = 1.32$ mg/m²



— 200 μ m

Acknowledgements

Prof. Juan M. Lopez (Arizona State)

Dr. Michael J. Vogel (RPI, Cornell)

Dr. Reza Miraghaie (RPI, Keck Institute & Claremont College)

Dr. Jonathan Leung (RPI)

Research funded by: NSF (CTS)

Seminar series sponsored by Los Alamos National Laboratories
through the Institute for Multiscale Materials Studies UCSB
(Directed by Prof. Bud Homsy)